

# Using Bayesian Statistics for Extraction of Parameters from Artificially Generated Data

Ege Sönmez

*Department of Physics, Bilkent University, Ankara, Turkey*

June 2024

## Abstract

This study employs Bayesian statistics for parameter extraction from artificially generated data, focusing on comparing the  $\Lambda$ CDM (Lambda - Cold Dark Matter) and MOND (Modified Newtonian Dynamics) models. Through Bayesian analysis, we aim to evaluate the effectiveness of these cosmological models in describing the universe's dynamics. The research contributes to the field by offering insights into the applicability of Bayesian methods for parameter estimation in complex cosmological models, thereby enhancing the understanding of underlying astronomical phenomena.

## 1 Introduction

The  $\Lambda$ CDM (Lambda - Cold Dark Matter) model and Modified Newtonian Dynamics (MOND) represent two foundational frameworks in cosmology, each proposing different mechanisms to explain observed phenomena in the universe such as galaxy rotation curves, the distribution of cosmic microwave background radiation, and large-scale structure formations.

This research will not explore the comprehensive theories of the  $\Lambda$ CDM and MOND models in depth. However, a brief introductory overview is essential for grounding the subsequent analysis. The primary focus of the investigation is on the application of Bayesian methods to data extraction. As such, some formulas, particularly those pertaining to the  $\Lambda$ CDM model, will be simplified and modified for the purposes of this study. The critical aspect to grasp is the data extraction process using Bayesian techniques and the numerical methods associated with this approach.

### 1.1 $\Lambda$ CDM Model

The  $\Lambda$ CDM model is based on the cosmological principle, which states that the universe is homogeneous and isotropic on large scales. It builds upon the framework of general relativity, with the Einstein field equations at its core:

$$R_{\mu\nu} - \frac{1}{2}g_{\mu\nu}R + g_{\mu\nu}\Lambda = \frac{8\pi G}{c^4}T_{\mu\nu}, \quad (1)$$

where  $R_{\mu\nu}$  is the Ricci curvature tensor,  $R$  is the Ricci scalar,  $g_{\mu\nu}$  is the metric tensor,  $\Lambda$  is the cosmological constant,  $G$  is the gravitational constant,  $c$  is the speed of light, and  $T_{\mu\nu}$  is the stress-energy tensor. [1]

The expansion of the universe is described by the Friedmann equations, derived from the Einstein field equations for a FLRW metric:

$$H^2 = \left(\frac{\dot{a}}{a}\right)^2 = \frac{8\pi G}{3}\rho - \frac{kc^2}{a^2} + \frac{\Lambda c^2}{3}, \quad (2)$$

$$\frac{\ddot{a}}{a} = -\frac{4\pi G}{3}(\rho + 3p/c^2) + \frac{\Lambda c^2}{3}, \quad (3)$$

where  $a(t)$  is the scale factor,  $H$  is the Hubble parameter,  $\rho$  is the total energy density of the universe,  $p$  is the pressure, and  $k$  describes the curvature of space.

The critical density,  $\rho_{\text{crit}}$ , necessary to close the universe, is defined as:

$$\rho_{\text{crit}} = \frac{3H^2}{8\pi G}, \quad (4)$$

and the density parameters for matter, dark energy, and radiation are given by:

$$\Omega_m = \frac{\rho_m}{\rho_{\text{crit}}}, \quad \Omega_\Lambda = \frac{\Lambda c^2}{3H^2}, \quad \Omega_r = \frac{\rho_r}{\rho_{\text{crit}}}, \quad (5)$$

leading to the critical equation of total density parameter:

$$\Omega_{\text{tot}} = \Omega_m + \Omega_\Lambda + \Omega_r = 1 - \frac{kc^2}{H^2 a^2}. \quad (6)$$

The  $\Lambda$ CDM model parameters are constrained through various observations, including the cosmic microwave background (CMB) anisotropies, supernovae type Ia luminosity distances, baryon acoustic oscillations, and large-scale structure surveys. [2]

To integrate the impacts of the  $\Lambda$ CDM model within the Newtonian gravitational framework for this analysis, we propose an altered version of the classical gravitational force equation as follows:

$$G \frac{m(M + \eta)}{r^2} = ma, \quad (7)$$

where  $\eta$  is an added term to account for the mass equivalent attributed to dark matter in the galaxy, which, despite not being directly observable through

electromagnetic means, influences the gravitational behavior of visible matter.

This adjustment allows for the inclusion of dark matter's gravitational effects into the Newtonian gravity equation without modifying the foundational law of gravity. The introduction of  $\eta$  accommodates the gravitational pull of unobservable dark matter on visible matter, reconciling the Newtonian description of gravity with galactic observations unexplained by visible matter alone.

While  $\eta$  predominantly covers the role of dark matter at galactic scales, the cosmological constant  $\Lambda$  from the  $\Lambda$ CDM model, symbolizing dark energy, is mainly addressed in the context of the universe's overarching structure and its accelerated expansion. In this study, our focus is primarily on applying Bayesian methods for data extraction and analysis. Hence, the presented equation serves as a simplified yet practical approach to include classical mechanics with cosmological phenomena for computational modeling and numerical analysis within the Bayesian statistical framework.

## 1.2 MOND

In contrast to dark matter hypotheses, Modified Newtonian Dynamics (MOND) posits a modification of Newton's second law at low accelerations to explain galactic rotation curves. The MOND equation is formulated as:

$$F_N = m\mu\left(\frac{a}{a_0}\right)a, \quad (8)$$

where  $F_N$  is the Newtonian force,  $m$  is the mass,  $a$  is the acceleration, and  $a_0$  is a characteristic acceleration below which MOND effects become significant. The function  $\mu(x)$ , known as the interpolating function, transitions between the Newtonian and MONDian regimes. Consistency with Newtonian mechanics is maintained as  $\mu(x) \rightarrow 1$  for  $x \gg 1$ , and the adherence to astronomical observations as  $\mu(x) \rightarrow x$  for  $x \ll 1$ . Two common forms of the interpolating function are the "simple" and "standard" interpolating functions:

$$\mu(x) = \frac{1}{1 + \frac{a_0}{a}}, \quad (9)$$

and

$$\mu(x) = \frac{1}{\sqrt{1 + \left(\frac{a_0}{a}\right)^2}}. \quad (10)$$

In the deep-MOND regime where  $a \ll a_0$ , the MONDian force law reduces to:

$$F_N = m\frac{a^2}{a_0}. \quad (11)$$

For a star or other object of mass  $m$  in circular orbit about a mass  $M$ , MOND predicts that:

$$\frac{GMm}{r^2} = m\left(\frac{v^2}{r}\right)^2, \quad (12)$$

which can be rearranged to give the relation for the rotational velocity:

$$v^4 = GMa_0. \quad (13)$$

This equation provides an explanation for the flat rotation curves observed in galaxies without invoking dark matter.

Through analysis of galactic rotation curves, Milgrom determined that the optimal value for the characteristic acceleration  $a_0$  in his formulation is approximately  $1.2 \times 10^{-10}$  meters per second squared. [3]

For the MOND aspect of this study, we will implement Equation (9) which is articulated as follows:

$$G\frac{Mm}{r^2} = m\left(\frac{1}{1 + \frac{a_0}{a}}\right)a, \quad (14)$$

This equation serves to encapsulate the modified dynamics proposed by MOND, effectively adjusting Newtonian gravitational predictions for systems experiencing accelerations below the threshold  $a_0$ . It addresses the anomalous rotation curves of galaxies without necessitating dark matter, by modifying the effective gravitational force at low accelerations. This modification is central to our analysis, enabling a comparative evaluation of gravitational models through the lens of Bayesian methods and numerical simulations.

## 2 Bayesian Approach

The Bayesian approach to statistical inference represents a paradigm shift from traditional frequentist statistics. It is particularly powerful in data interpretation and extraction due to its ability to incorporate prior knowledge and its flexibility in updating beliefs in light of new evidence.

At the heart of Bayesian statistics is Bayes' Theorem, which updates the probability for a hypothesis as evidence is accumulated. The theorem is articulated as:

$$P(\theta|X) = \frac{P(X|\theta) \cdot P(\theta)}{P(X)}, \quad (15)$$

where:

- $P(\theta|X)$  is the posterior probability of the parameter  $\theta$  after observing the data  $X$ .
- $P(X|\theta)$  is the likelihood of observing the data  $X$  given the parameter  $\theta$ .
- $P(\theta)$  is the prior probability of the parameter  $\theta$ , reflecting our knowledge about  $\theta$  before seeing the data.
- $P(X)$  is the evidence or the marginal likelihood of the data under all possible values of  $\theta$ .

In practice, Bayesian data analysis involves the following steps:

1. **Model Specification:** A statistical model that describes how data are generated is proposed. This includes defining the likelihood function  $P(X|\theta)$ .
2. **Prior Distribution:** Prior beliefs about the parameters are encoded in a prior distribution  $P(\theta)$ .
3. **Computation of the Posterior:** Using observed data, the posterior distribution  $P(\theta|X)$  is calculated, which combines the likelihood and the prior distribution.
4. **Inference:** Statistical inferences are made based on the posterior distribution. This could include estimating parameters, making predictions, and testing hypotheses.

The Bayesian method excels in situations where the amount of data is limited or the data is incrementally collected, as it allows for sequential updating of the posterior. It also provides a natural and coherent method for uncertainty quantification and decision making. [4]

## 2.1 Bayesian vs. Frequentist Approach

To provide context, the Bayesian approach can be contrasted with the frequentist approach as follows:

- **Frequentist:**
  - Views data as a repeatable random sample.
  - Regards underlying parameters as fixed and unknown constants.
  - Conducts inference by emphasizing long-run frequency properties of estimators.
- **Bayesian:**
  - Treats data as fixed and observed from the actual sample.
  - Considers parameters as uncertain quantities described by probability distributions.
  - Integrates prior information and updates parameter estimates as new data becomes available.

The Bayesian approach to statistical inference is widely applied in many fields due to its flexibility in incorporating prior information and its adaptability to updating information as new data is collected. It provides a comprehensive framework for understanding the probability and uncertainty inherent in complex data.

## 2.2 Metropolis-Hastings Algorithm

The Metropolis-Hastings algorithm is a cornerstone of modern Bayesian statistical computation. It allows for sampling from complex distributions by constructing a Markov chain that has the desired distribution as its equilibrium distribution.

## Algorithm Formalization

The Metropolis-Hastings algorithm proceeds as follows:

1. Initialize the algorithm with a starting point,  $x^{(0)}$ , which is a guess from the parameter space of the distribution we want to sample from.
2. For each iteration  $t = 1, 2, \dots, T$ :
  - (a) Generate a candidate sample  $x^*$  from a proposal distribution  $p(x^*|x^{(t-1)})$ .
  - (b) Compute the acceptance ratio  $\alpha$ , which is the probability of moving to the candidate sample:

$$\alpha(x^*, x^{(t-1)}) = \min \left\{ 1, \frac{P(x^*)p(x^{(t-1)}|x^*)}{P(x^{(t-1)})p(x^*|x^{(t-1)})} \right\},$$

where  $P$  is the target distribution we are trying to sample from.

- (c) Accept or reject the candidate sample:
  - With probability  $\alpha$ , accept the candidate and set  $x^{(t)} = x^*$ .
  - With probability  $1 - \alpha$ , reject the candidate and set  $x^{(t)} = x^{(t-1)}$ .

3. After a large number of iterations  $T$ , the set  $\{x^{(1)}, x^{(2)}, \dots, x^{(T)}\}$  is a sample from the distribution  $P$ .

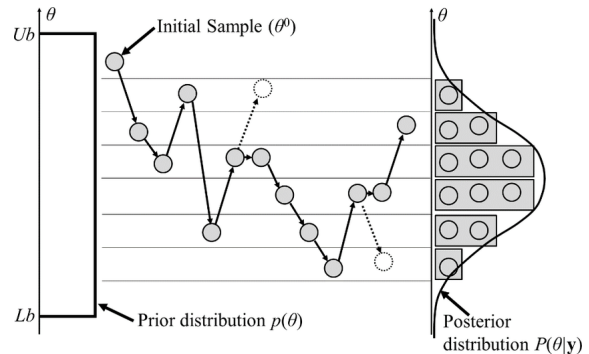


Figure 1: Flowchart of Metropolis - Hastings Algorithm [5]

The proposal distribution  $p$  is crucial for the efficiency of the algorithm. It must be chosen carefully to ensure that the Markov chain mixes well and that the acceptance rate is neither too low nor too high.

The Metropolis-Hastings algorithm is particularly useful for high-dimensional or otherwise complex probability distributions where direct sampling is not feasible. It is widely used in Bayesian data analysis to sample from posterior distributions, enabling the estimation of model parameters, predictions, and hypothesis testing.

### 3 Simulation

In the simulation section of this study, we will employ the Metropolis-Hastings (MH) algorithm to determine which theoretical model— $\Lambda$ CDM or MOND—better aligns with the artificially generated data.

#### 3.1 Preliminary Test of MH

As a preliminary step and to validate the functionality of the algorithm, including the accuracy of the acceptance ratios, we will first generate a series of samples ( $w$ ) based on classical Newtonian gravitation expressed as:

$$\frac{GMm}{r^2} = \frac{mv^2}{r}, \quad (16)$$

where the radial distance  $r$  is drawn from a normal distribution  $N(10, 4)$  and the mass  $M$  from  $N(5, 1)$ , scaled to Astronomical Units (AU), and 15,000 samples as per the methodology used by Banik et al [6]. Utilizing the generated angular velocities  $w$  and the normally distributed masses  $M$  and radial distances  $r$ , we will infer the posterior distributions of  $\eta$  in the  $\Lambda$ CDM model and  $a_0$  in the MOND model.

If the algorithm functions as anticipated, we expect these parameters to center around zero. This expectation is grounded in the assumption that substituting zero for these parameters in equation 7 and 14 reverts to classical Newtonian gravitation, reflecting the origin of our generated  $w$  values. The simulation's success will be measured by the proximity of inferred parameter values to this theoretical baseline.

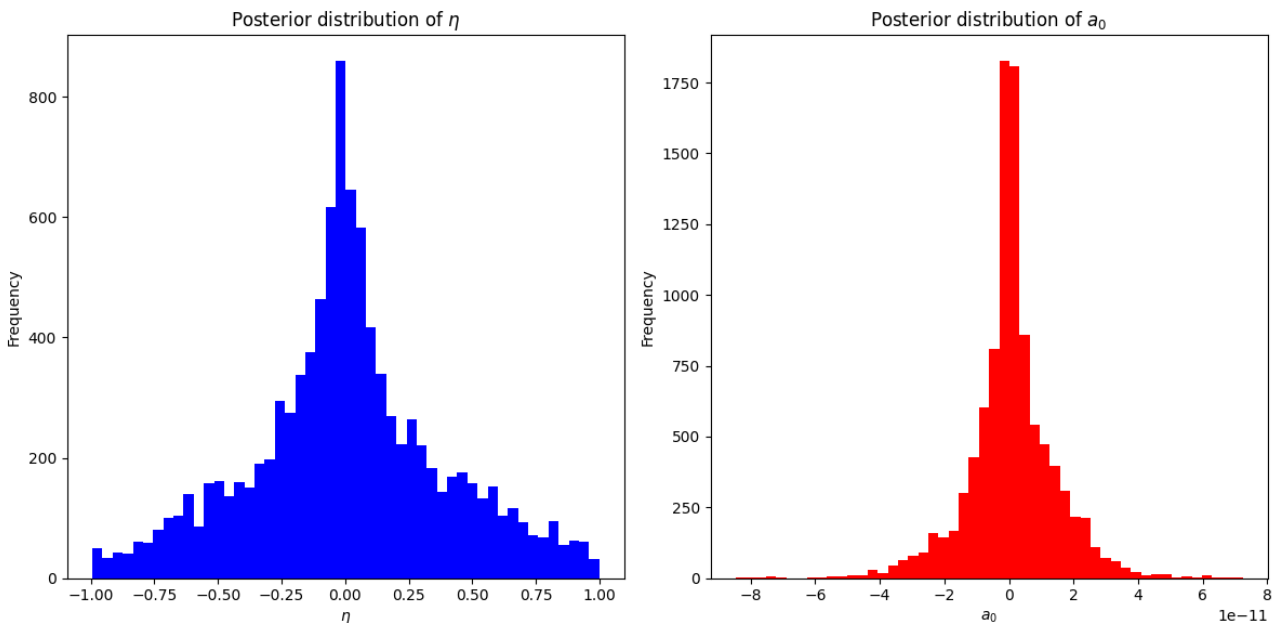


Figure 2: Posterior distributions of  $\eta$  and  $a_0$ , using 15000 samples of ( $w$ ) that are synthesized based on classical Newtonian dynamics.

The findings depicted in Figure 2 validate the functionality of the Metropolis-Hastings (MH) algorithm and the accuracy of the acceptance ratios. This is evidenced by the distributions of  $\eta$  and  $a_0$  centering around 0, aligning with our expectations for these parameters to mirror classical Newtonian dynamics.

### 3.2 Data Generation

Due to the inaccessibility of the GAIA dataset for this study, we will create our own data to mirror the GAIA dataset's characteristics closely. Despite being unconventional, this method aligns well with the challenges of astronomical data collection, like those seen with GAIA, and does not impact our study's focus on applying the Metropolis-Hastings (MH) algorithm. The synthesized data, designed to reflect GAIA's key features, is given in Figure 3.

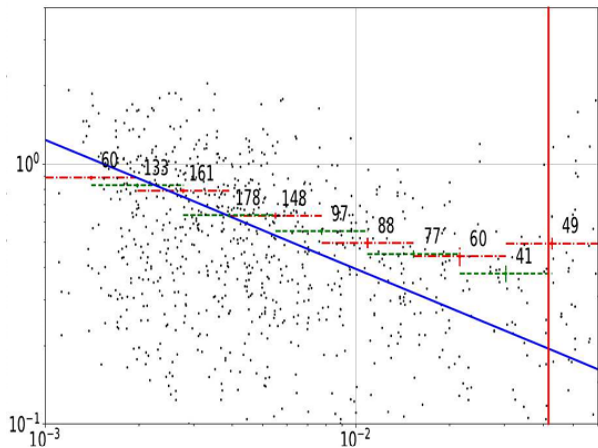


Figure 3: The data points reflect velocities (on the y-axis) against the distance ( $r$ ) between wide binary stars (on the x-axis) as derived from the GAIA dataset for approximately 400 pairs. [7]

Therefore, in the data generation phase, we will construct a baseline linear model and incorporate noise into it to closely resemble the observed data characteristics. Utilizing these synthesized samples, we will derive new distributions for both the velocities ( $v$ ) and distances ( $r$ ) between wide binary stars. The artificially generated samples are expected to display a pattern as the following:

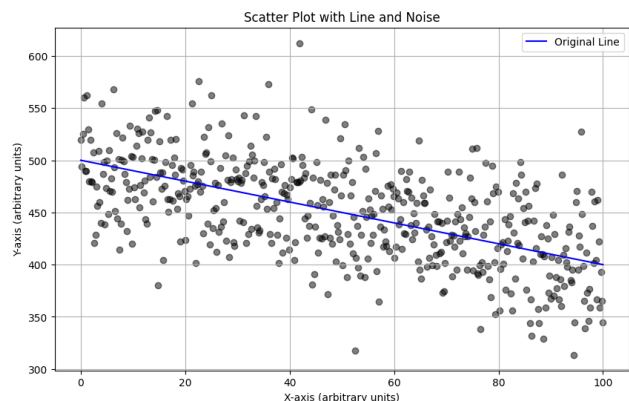


Figure 4: Artificially generated data (500 points) with the line equation  $y = -x + 500$  in arbitrary units.

For the data points generated by this linear model with added noise, there are two potential approaches for analysis. The data points can either be used di-

rectly or serve as inputs for the Metropolis-Hastings (MH) algorithm to create sample distributions for the posterior probabilities of  $\eta$  and  $a_0$ . By applying the MH algorithm to both the initial data generation and subsequently to infer the posterior distributions of  $\eta$  and  $a_0$ , we can achieve more accurate results. This dual application of MH enhances the precision of the acceptance ratios, thus refining the overall inference process. Consequently, the posterior distributions derived from the artificially created data points can effectively represent sample distributions of our target parameters, potentially yielding results with increased precision. The expected distribution pattern from such a process will resemble the following:

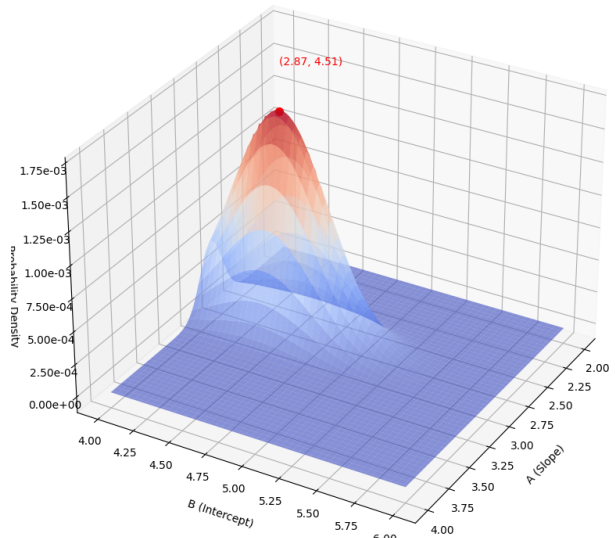


Figure 5: The posterior distribution derived from a model described by the equation  $y = 3x + 5$ , where standard normal noise with a standard deviation of  $\sigma = 2$  was applied, all measured in arbitrary units.

Thus, after adjusting the units for the probability densities of  $v$  and  $r$ , these can be utilized, or the synthesized data points can be directly employed without initially resorting to the Metropolis-Hastings algorithm.

### 3.3 Scaling

In our analysis, we scaled the variables in the Modified Newtonian Dynamics (MOND) equation to make calculations more manageable by using astronomical units. The original MOND equation is given by:

$$\frac{GM}{r} = \frac{v^2}{1 + \frac{a_0}{a}},$$

where  $a = \frac{v^2}{r}$ .

We introduce scaled variables by expressing the original variables in terms of their astronomical units

counterparts:

$$\begin{aligned} M &= \bar{M} \cdot M^*, \\ r &= \bar{r} \cdot r^*, \\ v &= \bar{v} \cdot v^*, \end{aligned}$$

where  $\bar{M}$ ,  $\bar{r}$ , and  $\bar{v}$  are the astronomical units for mass, distance, and velocity, respectively, and  $M^*$ ,  $r^*$ , and  $v^*$  are the dimensionless scaled variables.

The astronomical units used are:

$$\begin{aligned} \bar{M} &= 2 \times 10^{30} \text{ kg}, \\ \bar{r} &= 1.496 \times 10^{11} \text{ m}, \\ \bar{v} &= 29788.9 \text{ m/s}. \end{aligned}$$

Substituting the scaled variables into the MOND equation, we have:

$$\frac{G(\bar{M}M^*)}{\bar{r}r^*} = \frac{(\bar{v}v^*)^2}{1 + \frac{a_0}{\frac{(\bar{v}v^*)^2}{\bar{r}r^*}}}.$$

Dividing through by the astronomical units, we get:

$$\frac{G\bar{M}M^*}{\bar{r}r^*} = \frac{\bar{v}^2 v^{*2}}{1 + \frac{a_0 \bar{r}}{v^{*2} \bar{v}^2} r^*}.$$

Simplifying, we get:

$$\frac{M^*}{r^*} = \frac{v^{*2}}{1 + \left(\frac{a_0 \bar{r}}{\bar{v}^2}\right) \frac{r^*}{v^{*2}}}.$$

We define the scaled acceleration  $a_0^*$  as:

$$a_0^* = \frac{a_0 \bar{r}}{\bar{v}^2}.$$

Substituting  $a_0^*$  into the equation, we obtain:

$$\frac{M^*}{r^*} = \frac{v^{*2}}{1 + a_0^* \frac{r^*}{v^{*2}}}.$$

### 3.3.1 Summary of Scaling Transformations

To summarize, the scaling transformations applied are:

$$M^* = \frac{M}{\bar{M}}, \quad (17)$$

$$r^* = \frac{r}{\bar{r}}, \quad (18)$$

$$v^* = \frac{v}{\bar{v}}, \quad (19)$$

$$a_0^* = \frac{a_0 \bar{r}}{\bar{v}^2}. \quad (20)$$

These transformations allowed us to work with dimensionless quantities, simplifying the analysis and ensuring consistency in units across all calculations.

## 3.4 Method

This section details the methodology used to generate data based on the Modified Newtonian Dynamics

(MOND) model and to simulate the posterior distributions of parameters using the Metropolis-Hastings algorithm. The procedure involves generating synthetic data for star masses and distances, calculating velocities, and then estimating the parameters  $\eta$  and  $a_0$ .

The MOND model was utilized to generate synthetic data for analysis. The following steps were performed:

1. **Generating Distances:** Distances  $D$  were randomly generated in the range of 50 to 200 parsecs using a uniform distribution.

$$D = \text{uniform}(50, 200)$$

These distances were converted to meters ( $r_{\text{meters}}$ ) and astronomical units ( $R_{\text{AU}}$ ).

$$\begin{aligned} r_{\text{meters}} &= D \times 3.086 \times 10^{16}, \\ R_{\text{AU}} &= \frac{r_{\text{meters}}}{1.496 \times 10^{11}} \end{aligned}$$

2. **Generating Masses:** Star masses  $M_{\text{star}}$  were generated using a normal distribution with a mean ( $\mu_M$ ) of 0.8 and a standard deviation ( $\sigma_M$ ) of 0.2.

$$M_{\text{star}} \sim \mathcal{N}(0.8, 0.2)$$

These masses were converted to kilograms ( $M$ ) using the solar mass unit.

$$M = M_{\text{star}} \times 2 \times 10^{30}$$

3. **Calculating Velocities:** Velocities were calculated using the MOND model equation:

$$v = \sqrt{\frac{GM}{r} + \frac{\sqrt{GM}\sqrt{GM + 4a_0 r^2}}{r}} \div \sqrt{2}$$

### 3.4.1 Simulation Using the Metropolis-Hastings Algorithm

The Metropolis-Hastings algorithm was employed to estimate the posterior distributions of the parameters  $\eta$  and  $a_0$ . The process is outlined as follows:

1. **Initialization:** The algorithm was initialized with starting values for  $\eta$  and  $a_0$ .

$$\eta_0 = 0.1,$$

$$a_0 = 1 \times 10^{-11}$$

2. **Proposal Distributions:** New candidate values for  $\eta$  and  $a_0$  were generated using normal distributions centered around the current values.

$$\eta_{\text{proposal}} = \eta_{\text{current}} + \mathcal{N}(0, 0.5),$$

$$a_{0\text{proposal}} = a_{0\text{current}} + \mathcal{N}(0, 1 \times 10^{-11})$$

3. **Prior Probability:** A prior function was defined to ensure the proposed values were within the acceptable range.

$$\text{prior}(\eta, a_0) = \begin{cases} 1 & \text{if } -1 \leq \eta \leq 1 \text{ and } -1 \leq a_0 \leq 1, \\ 0 & \text{otherwise} \end{cases}$$

4. **Likelihood Function:** Likelihood functions for  $\eta$  and  $a_0$  were defined based on the model equations defined by the function  $\mathcal{L}(x)$ .

5. **Acceptance Criteria:** The acceptance of proposed values was determined using the acceptance ratio.

$$\alpha = \min \left( 1, \frac{\mathcal{L}(\eta_{\text{proposal}})\mathcal{L}(a_{0\text{proposal}})}{\mathcal{L}(\eta_{\text{current}})\mathcal{L}(a_{0\text{current}})} \right)$$

If the proposal was accepted, the new values were added to the sample; otherwise, the current values were retained.

6. **Iteration:** This process was repeated for a specified number of iterations (e.g., 50,000) to build the posterior distributions of  $\eta$  and  $a_0$ .

After generating data using the MOND model, the code was modified to generate data based on the Lambda Cold Dark Matter (CDM) model. The same Metropolis-Hastings algorithm was then applied to estimate the parameters for the CDM model. The resulting posterior distributions for both models were compared to evaluate their performance in describing the simulated data.

## 4 Results

The results obtained from the MOND generated data are presented below. Using the generated data, we applied the Metropolis-Hastings algorithm to estimate the posterior distributions of the parameters  $\eta$  and  $a_0$ . The goal was to assess the effectiveness of the MOND model in describing the simulated data.

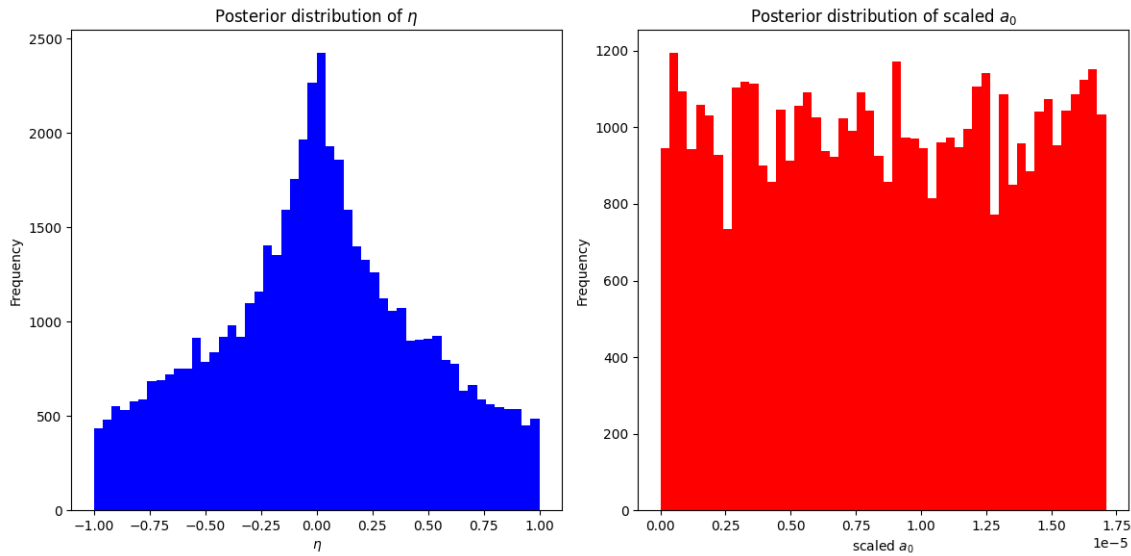


Figure 6: Posterior distributions of  $\eta$  and  $a_0 = 1.2 \times 10^{-10}$ , using 15000 samples of  $(v)$  that are synthesized based on MOND.

The data points of velocities against the distance is presented below.

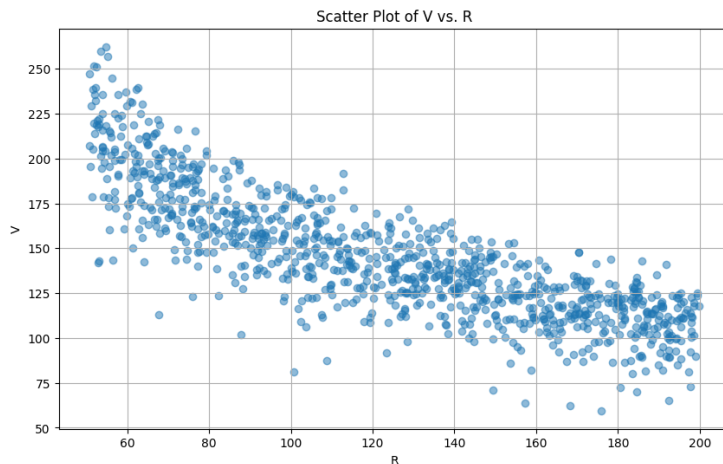


Figure 7: Velocity vs. Distance graph of MOND generated data.

Then, we generated data using the CDM model, which yielded the distributions below.

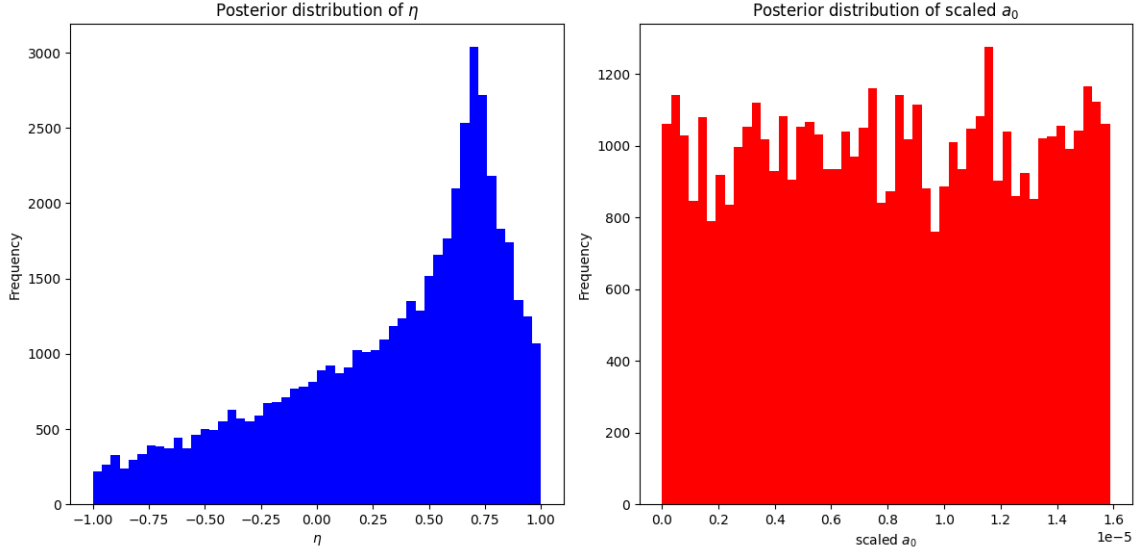


Figure 8: Posterior distributions of  $\eta = 0.7$  and  $a_0$ , using 15000 samples of  $(v)$  that are synthesized based on CDM.

The data points of velocities against the distance is presented below.

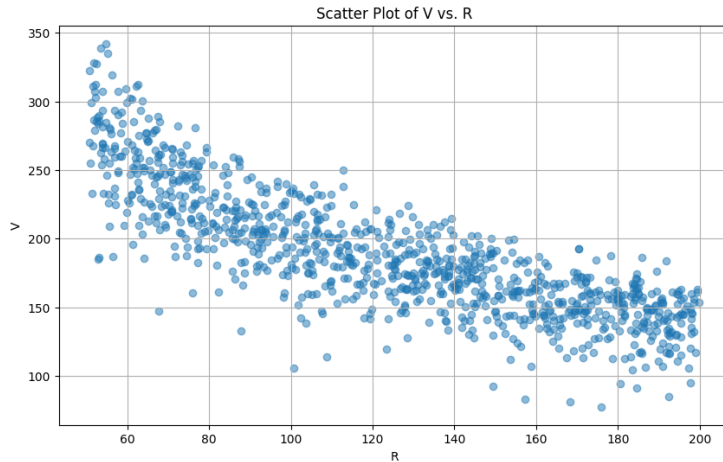


Figure 9: Velocity vs. Distance graph of CDM generated data.

## 5 Discussion

This section discusses the results obtained from the Bayesian analysis using the Metropolis-Hastings algorithm on data generated from Classical Newtonian, MOND, and CDM models. The goal is to evaluate the accuracy and reliability of parameter estimation for each model.

### 5.1 Classical Newtonian Generated Data

The analysis of data generated using the classical Newtonian model serves as a baseline for comparison. The posterior distributions for both  $\eta$  and  $a_0$  exhibit peaks at 0, as shown in Figure 2. This result is expected because when  $\eta = 0$  and  $a_0 = 0$ , the models

revert to classical Newtonian dynamics.

The sharp peak at 0 in the  $\eta$  distribution indicates that the Bayesian method accurately recovers the Newtonian dynamics without any modifications. These findings validate the functionality of the Metropolis-Hastings algorithm and its accuracy in estimating parameters from classical Newtonian generated data.

### 5.2 MOND Generated Data

The analysis of the data generated using the MOND model reveals significant insights into the behavior of the parameters  $\eta$  and  $a_0$ .

For the  $\eta$  parameter, the posterior distribution does not exhibit a sharp peak at 0, unlike the classical Newtonian case (Figure 6). This difference is attributable to the introduction of the parameter  $a_0 = 1.2 \times 10^{-10}$

in the MOND model, which alters the data generation method. Although  $a_0$  is small, its effects are clearly evident in the  $\eta$  distribution. The presence of  $a_0$  causes the distribution to spread, resulting in a less pronounced peak at 0. This observation highlights the influence of the  $a_0$  parameter in the MOND model and distinguishes it from the classical Newtonian dynamics, where  $\eta$  had a sharp peak at 0.

On the other hand, the posterior distribution of  $a_0$  shows a more uniform distribution between 0 and  $1.75 \times 10^{-5}$ . The order of magnitude of the distribution is correct, considering the scaling transformations applied during the analysis. However, the exact value of  $a_0 = 1.2 \times 10^{-10}$  could not be extracted precisely. This outcome could be due to the variance in the data and the relatively small effect that  $a_0$  has on the overall dynamics. Another possible reason is that the Metropolis-Hastings algorithm might skip the minima due to the small magnitude of  $a_0$ , and the fluctuations in the probability estimates might prevent the algorithm from converging to the correct parameter value.

In summary, while the MOND model effectively alters the  $\eta$  distribution, reflecting the impact of the parameter  $a_0$ , the precise extraction of  $a_0$  remains challenging. The uniform distribution of  $a_0$  suggests that further refinement of the data generation method or the algorithm might be necessary to improve the accuracy of parameter estimation.

### 5.3 CDM Generated Data

The case with the CDM generated data is somewhat similar to the MOND generated data but with distinct characteristics. Given  $\eta = 0.7$ , the algorithm successfully extracts this value, although the peak is not as sharp as in the classical case. The broader peak indicates some level of uncertainty, but overall, the parameter  $\eta$  is well captured by the algorithm.

However, the issue with the  $a_0$  parameter persists in the CDM case. The posterior distribution of  $a_0$  is uniformly distributed approximately around the same range as observed in the MOND generated data, be-

tween 0 and  $1.75 \times 10^{-5}$ . This uniform distribution suggests that the algorithm struggles to pinpoint the exact value of  $a_0$ , potentially due to the same reasons identified in the MOND case: the small magnitude of  $a_0$  relative to the data variance and the possibility of the algorithm skipping over the minima due to probability fluctuations.

## 6 Conclusion

In this study, we employed Bayesian statistics, specifically the Metropolis-Hastings algorithm, to extract parameters from artificially generated data using the MOND and CDM models. The results revealed distinct differences in the ability of these models to recover the expected parameters. The classical Newtonian model served as a baseline, demonstrating that the algorithm could accurately estimate parameters when the underlying dynamics are unaltered.

For the MOND generated data, the introduction of the parameter  $a_0$  led to a noticeable spread in the  $\eta$  distribution, reflecting the model's sensitivity to low accelerations. However, the  $a_0$  parameter proved challenging to estimate precisely, likely due to its small magnitude and the variance in the data. Similarly, in the CDM generated data, while the  $\eta = 0.7$  value was successfully extracted, the  $a_0$  parameter again showed a uniform distribution, indicating difficulties in pinpointing its exact value.

These findings highlight the strengths and limitations of both the MOND and CDM models in describing cosmological data. The MOND model effectively captures the impact of low accelerations, whereas the CDM model accurately represents the  $\eta$  parameter but struggles with  $a_0$ . Future research should focus on refining the data generation methods and improving the Bayesian algorithms to enhance parameter estimation accuracy. This study underscores the importance of methodological advancements in cosmological modeling and contributes to a deeper understanding of the dynamics governing our universe.

## References

- [1] N. Deruelle, J.-P. Uzan, and P. de Forcrand-Millard, *Relativity in Modern Physics*. Oxford University Press, 08 2018. [Online]. Available: <https://doi.org/10.1093/oso/9780198786399.001.0001>
- [2] K.-H. Chae, "Breakdown of the newton-einstein standard gravity at low acceleration in internal dynamics of wide binary stars," *The Astrophysical Journal*, vol. 952, no. 2, p. 128, jul 2023. [Online]. Available: <https://dx.doi.org/10.3847/1538-4357/ace101>
- [3] M. Milgrom, "A modification of the newtonian dynamics - implications for galaxies," *Astrophysical Journal*, vol. 270, pp. 365–370, Jul 1983.
- [4] R. T. Cox, "Probability, Frequency and Reasonable Expectation," *American Journal of Physics*, vol. 14, no. 1, pp. 1–13, 01 1946. [Online]. Available: <https://doi.org/10.1119/1.1990764>
- [5] L. Tierney, "Markov Chains for Exploring Posterior Distributions," *The Annals of Statistics*, vol. 22, no. 4, pp. 1701 – 1728, 1994. [Online]. Available: <https://doi.org/10.1214/aos/1176325750>

- [6] I. Banik, C. Pittordis, W. Sutherland, B. Famaey, R. Ibata, S. Mieske, and H. Zhao, “Strong constraints on the gravitational law from Gaia DR3 wide binaries,” *Monthly Notices of the Royal Astronomical Society*, vol. 527, no. 3, pp. 4573–4615, 11 2023. [Online]. Available: <https://doi.org/10.1093/mnras/stad3393>
- [7] X. Hernandez, “Internal kinematics of Gaia DR3 wide binaries: anomalous behaviour in the low acceleration regime,” *Monthly Notices of the Royal Astronomical Society*, vol. 525, no. 1, pp. 1401–1415, 08 2023. [Online]. Available: <https://doi.org/10.1093/mnras/stad2306>

## 7 Appendix

Python code for the simulation.

```
import numpy as np
import matplotlib.pyplot as plt

np.random.seed(42)

G = 39.5
eta = 0.7
D = np.random.uniform(50, 200, 1000)
r_meters = D * 3.086e+16
r_au = 1.496e11
m_au = 2e30
v_au = 29788.9
a_0 = 1.2e-10

n_points = 1000
mu_M = 0.8
sigma_M = 0.2

M_star = np.random.normal(mu_M, sigma_M, n_points)
M = M_star * m_au
R_star = r_meters / r_au

plt.figure(figsize=(10, 6))
plt.scatter(M_star, R_star, alpha=0.5)
plt.xlabel('M_star')
plt.ylabel('R_star')
plt.title('Scatter Plot of M_star vs. R_star')
plt.grid(True)
plt.show()

r = r_meters
v = np.sqrt((G * M) / r + (np.sqrt(G) * np.sqrt(M) * np.sqrt(G * M + 4 * a_0 * r**2)) / r) / np.sqrt(2)
v_star = v / v_au

a=(v_star**2/R_star)/(a_0 * r_au / v_au**2)

plt.figure(figsize=(10, 6))
plt.plot(a)
plt.xlabel('')
plt.ylabel('')
plt.title('Scr')
plt.grid(True)
plt.show()

plt.figure(figsize=(10, 6))
plt.scatter(D, v_star, alpha=0.5)
plt.xlabel('R')
plt.ylabel('V')
plt.title('Scatter Plot of V vs. R')
plt.grid(True)
plt.show()

def prior(eta, a_0):
```

```

    return 1 if -1 <= eta <= 1 and -2 <= a_0 <= 2 else 0

def likelihood_eta(eta, R, v, M):
    lhs = G * M * (1 + eta) / R**2
    rhs = v**2 / R
    eq_1_error = np.sum((lhs - rhs)**2)
    return np.exp(-0.5 * eq_1_error), eq_1_error

def likelihood_a_0(a_0, R, v, M, r_au, m_au, v_au):
    lhs = (M / m_au) / (R / r_au)
    rhs = (v**2 / v_au**2) / (1 + (a_0 * r_au / v_au**2) * ((R / r_au) / (v**2 / v_au**2)))
    eq_2_error = np.sum((lhs - rhs)**2)
    return np.exp(-0.5 * eq_2_error), eq_2_error

def metropolis_hastings(iterations, R, v, M, r_au, m_au, v_au):
    eta_samples = [0.1]
    a_0_samples = [1e-11]
    for _ in range(iterations):
        eta_current = eta_samples[-1]
        a_0_current = a_0_samples[-1]

        eta_proposal = eta_current + np.random.normal(0, 0.5)
        a_0_proposal = a_0_current + np.random.normal(0, 1e-11)

        if prior(eta_proposal, a_0_proposal):
            _, eq_1_error_current = likelihood_eta(eta_current, R, v, M)
            _, eq_2_error_current = likelihood_a_0(a_0_current, R, v, M, r_au, m_au, v_au)

            _, eq_1_error_proposal = likelihood_eta(eta_proposal, R, v, M)
            _, eq_2_error_proposal = likelihood_a_0(a_0_proposal, R, v, M, r_au, m_au, v_au)

            if eq_1_error_proposal < eq_1_error_current or eq_2_error_proposal < eq_2_error_current:
                eta_samples.append(eta_proposal)
                a_0_samples.append(a_0_proposal)
            else:
                eta_samples.append(eta_current)
                a_0_samples.append(a_0_current)
        else:
            eta_samples.append(eta_current)
            a_0_samples.append(a_0_current)

    return eta_samples, a_0_samples

eta_samples, a_0_samples = metropolis_hastings(50000, r_meters, v, M, r_au, m_au, v_au)

a_0_scaled_samples = [a_0 * r_au / v_au**2 for a_0 in a_0_samples]

plt.figure(figsize=(12, 6))
plt.subplot(1, 2, 1)
plt.hist(eta_samples, bins=50, color='blue')
plt.title('Posterior distribution of  $\eta$ ')
plt.xlabel('$\eta$')
plt.ylabel('Frequency')

plt.subplot(1, 2, 2)
plt.hist(a_0_scaled_samples, bins=50, color='red')
plt.title('Posterior distribution of scaled  $a_0$ ')
plt.xlabel('scaled  $a_0$ ')
plt.ylabel('Frequency')

```

```
plt.tight_layout()  
plt.show()
```